CIWEM Chartered Institution of Water and Environmental Management **WILEY** Journal of Flood Risk Management

ORIGINAL ARTICLE

Dynamic downscaling based on weather types classification: An application to extreme rainfall in south-east Japan

J.-F. Vuillaume[1,2,3] ⓘ | S. Hearth[1,4]

[1]United Nations University, Institute for the Advanced Study of Sustainability, Global change and sustainability department UNU-IAS, Tokyo, Japan

[2]Japan Agency for Marine-Earth Science and Technology (JAMSTEC), Department of Integrated Climate Change Projection Research (IcliP), Yokohama Institute for Earth Sciences, Yokohama, Japan

[3]University of Tokyo, IIS Komaba, Global Hydrology and Water Ressources Engineering, Tokyo, Japan

[4]Ministry of Megapolis and Western Development, Government of Sri Lanka, Colombo, Sri Lanka

Correspondence
Jean-Francois Vuillaume, United Nations University Institute for the Advanced Study of Sustainability, UNU-IAS, 5-53-70 Jingumae, Shibuya-ku, Tokyo 150-8925, Japan.
Email: vuillaume@student.unu.edu

Optimisation physical scheme for weather forecast systems is an essential part of the development of efficient real-time weather forecasts. This research examines the use of weather type to cluster and to optimise the physical scheme of numerical weather prediction systems in the south-east coast of Japan in the Tokyo area. In this study, we calibrated and validated physical schemes by the observed rainfall at gauge stations around Tokyo, we have classified these per weather circulation. We used 24 ensemble members and 20 heavy rainfall events classified in 4 weather types to validate the scheme. The physical scheme ensemble construct by the association of micro-physics, cumulus, planetary boundary and radiative scheme and then, simulated with the weather research and forecasting model. We observed limited physical scheme variability for a pool of station within a weather type cluster. However, it shows large variations among stations. Then, we computed the rainfall Cumulative Probability Distribution Function curves which indicated wide differences. It suggests that clustering presents interesting properties. The results permitted (a) the selection of an optimal physical scheme per weather type, (b) the development of bias correction curve specific to weather type and (c) the evaluation the spatial distribution of regional bias correction.

KEYWORDS
forecasting and warning, Japan, meteorology, modelling, precipitation, weather types

1 | INTRODUCTION

The south-east coast of Japan around the region of Tokyo (called Kanto/Koshin region) is a largely urbanised area that is subject to heavy rains and strong winds resulting from different mechanisms such as tropical cyclones (Hayasaki & Kawamura, 2012) events and westerly winds. In the winter (DJF), the Siberian high developed. NW wind prevailed bringing sunny sunshine downstream of mountain area with occasional snowfall. In spring (MAM), the migration of cyclones that alternately move eastward across Japan. The temperature rise in the region of Tokyo and anticyclone systems installed during the second half of spring. During early June and middle July, rainy season (called Baiu) appended

caused by stationary front that forms where warm maritime tropical air mass meets cool air from the maritime air masses. Largest rainfall occurred in September due to active autumn rain front and tropical cyclones. In October, frequent anticyclone brings sunny condition in the Kanto area. Cold northwesterly flows across Japan increase in November (From JMA, 2017 Climate of Kanto/Koshin district).

The open source software weather research and forecasting (WRF), used for the dynamic downscaling method, is a popular dynamic downscaling model used for operational weather forecast and regional climate modelling (Skamarock et al., 2008). One of the core challenges of dynamical downscaling forecast set-up is the selection of the physical schemes according to the location, scale,

geography and weather events. In this paper, we focus on an ensemble of physically based parametrisation to simulate several extreme weather events in the south-east of Japan.

The regional dynamic downscaling method is a nested method to increase resolution and physical-based modelling of numerical weather prediction (NWP). It mainly consists of increasing the resolution of the simulation grid while using the boundaries of global forecast models and using the potential of physical scheme parametrisation. It gives a better capture of large scale processes such as hurricanes and allow local scale physical phenomena such as convective systems. Hence, it also allows the use of full physically based modelling schemes such as convective systems or cumulus and avoids parametrisation elements.

The optimisation of physical schemes is a standard method for regional weather forecast The experiments conducted by Jankov et al., (2005) used 18 ensemble members with a 12 km model resolution. The ensemble was created by the use of three microphysics (mp) parametrisations, two planetary boundary conditions (pbl) parametrisation and three cumulus (cu) parametrisation. Eight mesoscale convective systems were investigated during warm season over the South Central United States of America. The results confirmed the importance of the cu over the pbl scheme for rainfall sensitivity but also mentioned the need for different bias correction for various configurations.

A series of studies from Evans et al., (2012), Ji et al., (2014) and Gilmore et al., (2016) investigated the optimisation of a physics ensemble over the East coast of Australia for extra-tropical low-pressure associated with heavy rainfall. All of them used 36 ensemble members, and a nested domain was used with a 50 and 10 km resolution. Evans et al. (2012) concluded that none of the members was found to be the best of the four heavy rainfall investigated. But, it was possible to identify groups of model with the best performance. The authors advised for the combination of the Mellor-Yamada-Janjic (MYJ) planetary boundary layer scheme and the Betts-Miller-Janjic cumulus scheme (BMJ). Ji et al. (2014) extended the study, they used eight events and started to identify events in classes or cluster such as "lows in westerlies", "Easterly trough low", "decaying cold front", "Inland trough low", "Extra tropical cyclone" and "Wave on a front low". The authors stressed out the importance of ensemble average over a medium performance of a single scheme to obtain improvement in both spatial representation and quantity of rainfall. Finally, Gilmore et al. (2016) focused on a specific extreme event on the south-east coast of Australia and optimised scheme for the single June 8, 2007 cyclone event. In their experiments, the potentials of hourly rainfall forecasts was investigated and highlight that, cumulus and planetary boundary layer found to be the cause of the largest difference between physical schemes.

Other authors focused on specific categories of events such as tropical cyclone. Islam et al. (2015) used a 12 ensemble member with a 5 km resolution focused on the West Pacific Ocean. The authors concluded that, none of the schemes could be identified as optimal one but, cumulus scheme was designed as the most sensitive to rainfall intensity prediction to target the general rainfall underestimation of the system. Several researchers already mentioned the potential in classifying weather events by their categories but, without using automatic classification such as weather type. Furthermore, Jankov et al. (2005) already highlighted the need of appropriate bias correction associated with particular physical schemes association.

Classification of weather types is a well-described method mainly used in climate study rather than weather forecast optimisation. It is an adequate and powerful method to obtain, daily regular and automatic weather classification day by day (Rousi et al., 2014), that can be computed over a numerical grid. Therefore, it can be used to obtain significant statistical classification that characterise weather events. Moreover, Weather classification can extract finer detail than average temperature or rainfall parameters. Furthermore, the classification can be used for climate or weather system to obtain information on particular weather conditions. While classification methods can differ, weather type classification result presented a convenient limited number of members (Huth et al., 2008) that are characteristics of particular weather conditions. It has various uses domains of application such as cyclone hazards and air pollution, climatology and flood prevention. Hence, weather typing contained an association of parameters which summarised air mass specificity at different heights (typically 200, 500 and 925 hPa). Therefore, it can be related to synoptic scale condition (Bower et al., 2007; Riediger & Gratzki, 2014). In addition to wind direction, further parameters classifications can be combined such as the rainfall cumulative, the sunshine duration, relative humidity and minimal and maximal temperatures.

The Lamb weather type (LWT) by Lamb (1972) and the Grösswetterlagen catalogues (Hess & Brezowsky, 1952) based on pressure were the earliest tentative of weather classification based on physical parameters. In addition to this systematic classification, more subjective classifications were conducted by Jones et al., (1993) that prefigured the weather type approach as a semi-subjective approach. For the LWT, the indices computation used six different parameters, the southerly flow (SF), the westerly flow (WF), the total flow (F), the southerly shear vorticity (ZS), the westerly shear vorticity (ZW) and the total shear vorticity (Z). Overall, the indices can be derived from the mean sea level pressure (MSLP) measurements on a 16 points grid system with about 5–10 latitude–longitude spacing. Several authors have investigated the use of weather type in different
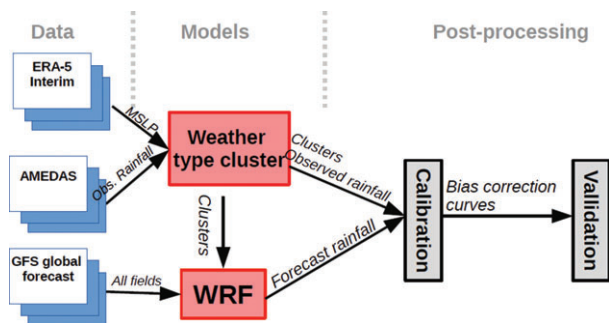
FIGURE 1 Shematic of the research framework. We highlight the data sets used (white-blue), the models (red boxes), and post-processing of calibration/validation (Grey boxes). ERA, European Re-Analysis; GFS, Global Forecast System; AMEDAS, Automated Meteorological Data Acquisition System; NOAA, National Oceanic and Atmospheric Administration; JMA, Japanese Meteorological Agency

regions with similar results showing the potential to improve weather classification for climate modelling such as Baltaci et al., 2014; Calvo et al., 2012; Kenawy et al., 2014; Lee & Sheridan, 2012; Riediger and Gratzki, 2014.

In this study, we investigated the potential of using weather type approach with dynamical downscaling scheme optimisation as illustrated by the Figure 1. We used ERA-40 Interim combined with the Automatic AMEDAS to classify weather type. Then, for each weather type, we produced an ensemble of forecasts with different associations of the planetary boundary, micro-physics, cumulus and radiative cumulus schemes for the cyclone, hybrid, westerly and north-westerly wind weather types. We created a 24 multi-physics ensemble using 2 pbl, 2 cu, 3 mp and 2 radiation (ra) schemes that we validated against rainfall station observations. A downscaling resolution of 27 and 9 km (Figure 2) was chosen because of the downscaling ratio that, allows cumulus scheme parametrisation to operate (i.e. <10 km).

This paper focuses on the statistical characterisation performance of the skill of various WRF configurations to simulate extreme events in the region of Tokyo. As such, the evaluations are performed over 75 observations stations which cover the region surrounding Tokyo. We used Japan as an illustration of the weather type "clustering-bias" correction method divided into 25 observations stations for calibration and 50 stations for validation, mostly centralised on the south east side of Japan in the area of weather type grid computation. Our study specifically targets heavy rainfall event.

The Section 2 gives a description of the data sets used in the study. The weather type method, the WRF model set-up and the bias correction method are all presented in Section 3. In the Section 4, the results are described and then, discussed in Section 5 with the methods used for bias correction and weather type selection.

2 | DATA: OBSERVATION AND FORECAST DATA

We use two on-line source data sets for our analyses: (a) the Automated Meteorological Data Acquisition System (AMEDAS) provided by the Japanese Meteorological Agency (JMA); (b) the ECMWF Re-Analysis interim data (ERA-interim) by the European Centre for Middle-range Weather Forecast. We compiled the period of availability of the data set in Table 1. The names and coordinates (lat-lon) of the station used are presented in Tables 2 and 3 with their name and latitude/longitude coordinates and localised Figure 3 with the WRF forecast grid. The AMEDAS is a network of automatic gauge station spread over Japan with an average density of one station per 17 km^2 provided by the JMA. The ERA-interim data is one of the global gridded data sets that provide MSLP in a concise manner similarly to the National Center for Environmental Protection (NCEP, USA) or the Japanese Re-Analysis (JMA, Japan).
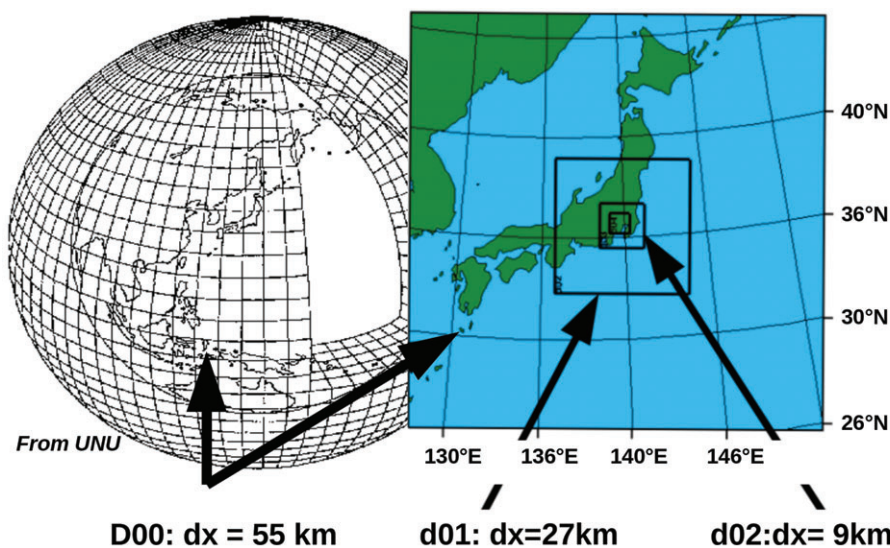

FIGURE 2 Illustration of the dynamic downscaling nested domain. The Global Forecast System, GFS, is 0.5° resolution while the domain 1 and 2 are 27 and 9 km respectively

TABLE 1 Available data-set used for the study

Data set	Provider	Date available	Duration (years)
ERA40-interim	ECMWF	January 01, 1979 to March 31, 2016	38
GFS	NOAA	October 10, 2006 to October 15, 2016	11
AMEDAS	JMA	January 01, 1978 to December 31, 2016	39

Note. AMEDAS = Automated Meteorological Data Acquisition System; ECMWF = European Center for Medium-Range Weather Forecasts; ERA = European Re-Analysis; GFS = Global Forecast System; JMA = Japanese Meteorological Agency; NOAA = National Oceanic and Atmospheric Administration.

3 | METHODS

3.1 | Weather type classification

The computation of weather type can be achieved by either subjective or automatic weather pattern determination. We use the MSLP as part as the ERA40-interim data to define weather types. The German Weather Agency based on LWT (Lamb, 1972) defined types classification. The method required the computation of the six parameters to allow the determination of eight purely wind direction and two types based on vorticity intensity. Also, a "hybrid" label is defined when a clear difference between purely laminar flow and vorticity was not identified. Trigo and

TABLE 2 Name (English translation and original Kanji name from JMA database) and location of the calibration stations

Station name	Japanese Kanji name (JMA database)	Longitude	Latitude
Shizuoka	静岡	138.4	36.0
Ajiro	網代	139.1	35.0
Mishima	三島	138.9	35.1
Ikawa	井川	138.2	35.2
Omaezaki	御前崎	138.2	34.6
Yokohama	横浜	139.7	35.4
Odawara	小田原	139.2	35.3
Miura	三浦	139.6	35.2
Tsujido	辻堂	139.5	35.3
Sagamiko	相模湖	139.2	35.6
Tokyo	東京	139.8	35.7
Edogawa Linhai	江戸川臨海	139.9	35.6
Ome	青梅	139.3	35.8
Ogouchi	小河内	139.1	35.8
Fuchu	府中	139.5	35.7
Chiba	千葉	140.1	35.6
Tateyama	館山	139.9	35.0
Katsuura	勝浦	140.3	35.2
Abiko	我孫子	140.1	35.9
Choshi	銚子	140.9	35.9
Kumagai	熊谷	139.4	36.2
Tokorozawa	所沢	139.4	35.8
Chichibu	秩父	139.1	36.0
Kuki	久喜	139.6	36.1
Koshigaya	越谷	139.8	35.9

Note. JMA = Japanese Meteorological Agency.

TABLE 3 Name (English translation and original Kanji name from JMA database) and location of the validation stations

Station name	Japanese Kanji name (JMA database)	Longitude (deci)	Latitude (deci)
Shizuoka Airport	静岡空港	138.2	34.8
keyhole	大山	138.3	35.1
Mikura	三倉	137.9	35.0
Shimizu	梅ケ島	138.3	35.2
Fuji	富士	138.7	35.2
Soil fertiliser	土肥	138.9	34.9
Amenroyama	天城山	139.0	34.9
Hakone	箱根	139.0	35.2
Lake Tanzawa	丹沢湖	139.0	35.4
Lake Sagami	相模湖	139.2	35.6
Hiratsuka	平塚	139.3	35.3
Sagamihara Central	相模原中央	139.4	35.6
Enoshima	江ノ島	139.5	35.3
Hiyoshi	日吉	139.7	35.6
Ozawa	小沢	139.1	35.7
Chofu	調布	139.5	35.7
Setagaya	世田谷	139.6	35.6
Haneda	羽田	139.8	35.6
Nerima	練馬	139.6	35.7
Three peaks	三峰	138.9	35.9
Kamiyoshida	上吉田	139.0	36.1
Urasan	浦山	139.1	35.9
Tokigawa	ときがわ	139.2	36.0
Hanno	飯能	139.3	35.8
Konosu	鴻巣	139.5	36.1
Saitama	さいたま	139.6	35.9
Sawan	鋸南	139.8	35.1
Otaki	大多喜	140.2	35.3
Kisarazu	木更津	139.9	35.4
Mobara	茂原	140.3	35.4
Funabashi	船橋	140.0	35.7
Narita	成田	140.4	35.8
Tōzo	東庄	140.7	35.8
Bando	坂東	139.9	36.0
Edogizu	江戸崎	140.3	36.0
Joso	常総	140.0	36.1
Tsuchiura	土浦	140.2	36.1
Kogi	門井	140.0	36.3
Minori	美野里	140.3	36.2
Furukawa	古河	139.7	36.2
Hokota	鉾田	140.5	36.2
Koseki	古関	138.6	35.5
Fuji Mountain	富士山	138.7	35.4
Katsunuma	勝沼	138.7	35.7
In the mountains	山中	138.8	35.4
Kawaguchiko	河口湖	138.8	35.5
Otsuki	大月	138.9	35.6
Uenohara	上野原	139.1	35.6

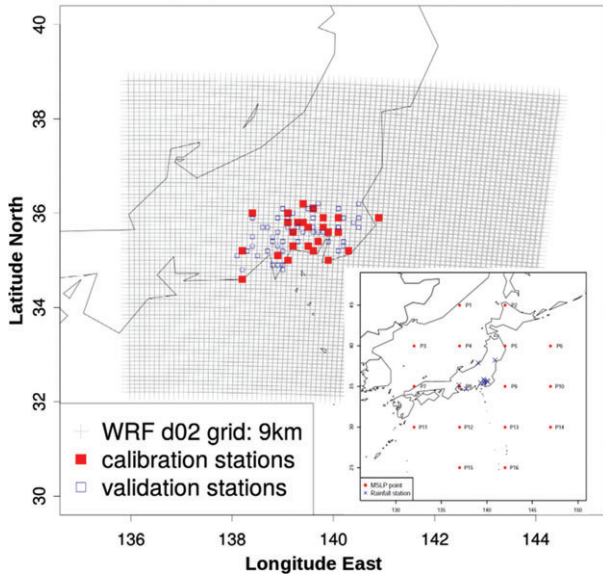*Note.* JMA = Japanese Meteorological Agency.

FIGURE 3 Regional forecast grid and weather stations locations used for the calibration of optimal scheme and the validation. Smaller Figure indicated the location of the mean sea level pressure (MSLP) grid points used for weather type computation. The names of the validation station were omitted due to space limitation

TABLE 4 Summary of classification of weather type clustering: purely directional, cyclonic, anticyclonic and hybrid

Class	Criteria
Purely directional (SE, E, NE, N, NW, W, SW, S)	$\|Z\| < F$
Cyclonic	$\|Z\| > 2F$, $Z > 0$
Anticyclonic	$\|Z\| > 2F$, $Z < 0$
Hybrid cyclonic and hybrid anti-cyclonic	$F < \|Z\| < 2F$

DaCamara (2000) set the six parameters (Equations (1)–(6)) needed for the weather type determination such as the Southern Flow (SF), the Westerly Flow (WF), the Westerly Shear Vorticity (ZW), the Southerly Shear Vorticity (ZS), the Resultant Flow (RF) and the Total Shear Vorticity (Z).

$$SF = 1.35 \frac{1}{4}[(p_5 + 2p_9 + p_{13}) - \frac{1}{4}(p_4 + 2p_8 + p_{12})] \quad (1)$$

$$WF = \left[\frac{1}{2}(p_{12} + p_{13}) - \frac{1}{2}(p_4 + p_5)\right] \quad (2)$$

$$ZW = 1.12 \frac{1}{2}[(p_5 + p_{16}) - \frac{1}{2}(p_8 + p_9)] \\ - 0.91 \frac{1}{2}[(p_8 + p_9) - \frac{1}{2}(p_1 + p_2)] \quad (3)$$

$$ZS = 0.85 \left[\frac{1}{4}(p_6 + 2p_{10} + p_{14}) - \frac{1}{4}(p_5 + 2p_9 + p_{13})\right] \\ - \frac{1}{4}[(p_4 + 2p_8 + p_{12}) + \frac{1}{4}(p_3 + 2p_7 + p_{11})] \quad (4)$$

$$RF = \left(WF^2 + SF^2\right)^{0.5} \quad (5)$$

$$Z = (ZS + ZW) \quad (6)$$

where p_1, p_2 ... p_{16} indicates the pressure points which are used to compute the weather type categories (el Kenawy et al., 2014). Then, pressure grid is defined with a 5° resolution between the coordinates 132°–147°E and 25°–45°N, for the period 1979–2016, and computed daily. The criteria used are summarised in Table 4.

As mentioned early, the flow strength (F), the vorticity (Z) and the mean direction (D) are computed from the pressure points. Then, we can determine if the weather type is mainly purely directional (N, NW, W, SW, S, SE and E) if it present a strong vorticity component cyclonic or anticyclonic) or if none of those categories ("Hybrid") as
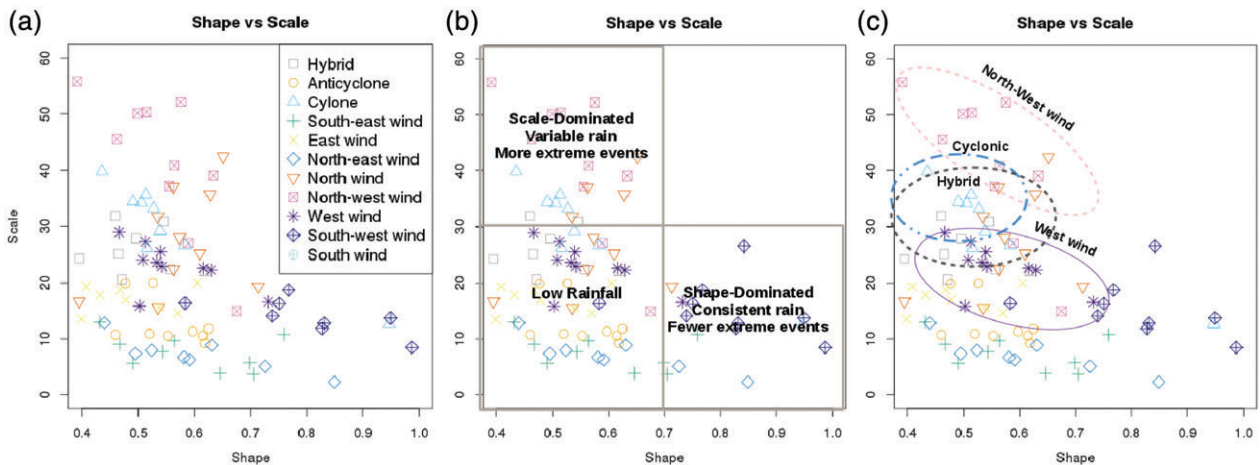

FIGURE 4 Cluster classification of rainfall retrieved in Automated Meteorological Data Acquisition System for the 10 study stations in Japan during the period 1979–2014. (a) Shape vs. scale plot of rainfall events for each station per weather type. (b) Interpretation of the rainfall type from a majority of extreme events towards fewer events. (c) Illustration of the clusters, where a cluster may enclose several cities (Vuillaume & Herath, 2016)
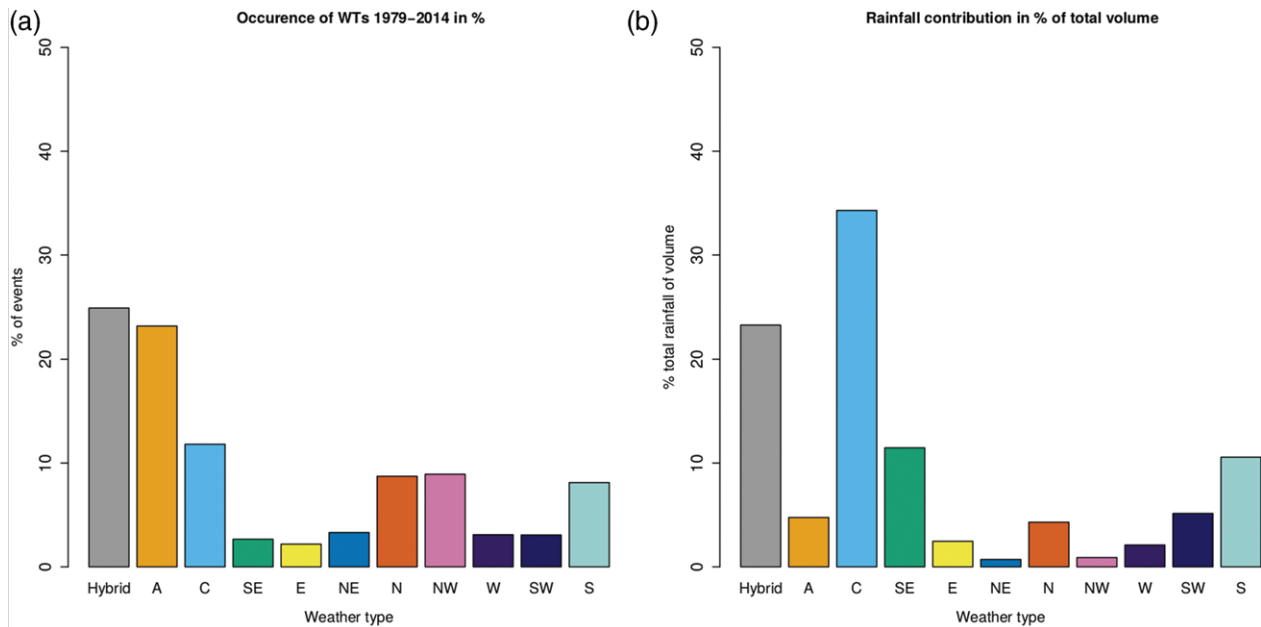
FIGURE 5 (a) Occurrence of weather types in Tokyo for 1979–2014. (b) Rainfall for each weather type as a percentage of the total in Tokyo. Hybrid corresponds to a system with a circulation flow between purely directional flow and shear flow (Vuillaume & Herath, 2016)

described by Jenkinson and Collison (1977). Previously, we evaluated the shape and scale signatures (Figure 4) of extreme rainfall events for 11 major urban area in south-east Japan as illustrated by the Figure 3. The computation of weather type in this region indicates that only cyclonic, hybrid, northwesterly and westerly are associated with heavy rainfall and represents potential clusters of rainfall pattern in term of scale and shape signatures (Figure 4). The results determine the most important weather type associated with extreme events in this area (Vuillaume & Herath, 2016). Therefore, we consider the cyclone (C), the hybrid

(H), the northwesterly (NW) wind and the westerly (W) wind.

We illustrate the summary of the results of the weather type determination in Figures 5 and 6. Figure 5 illustrates the distribution of weather type event (Figure 5a) and their contribution in percentage of water volume by type of weather type (Figure 5b). Therefore, cyclone, hybrid, south and southwesterly were identified as the major contribution of rainfall in volume for Tokyo station. Furthermore, our results indicate that cyclonic, hybrid, northwesterly and westerly types are associated with >100 and >150 mm/day heavy rainfall event in the South East region of Japan (Figure 6).
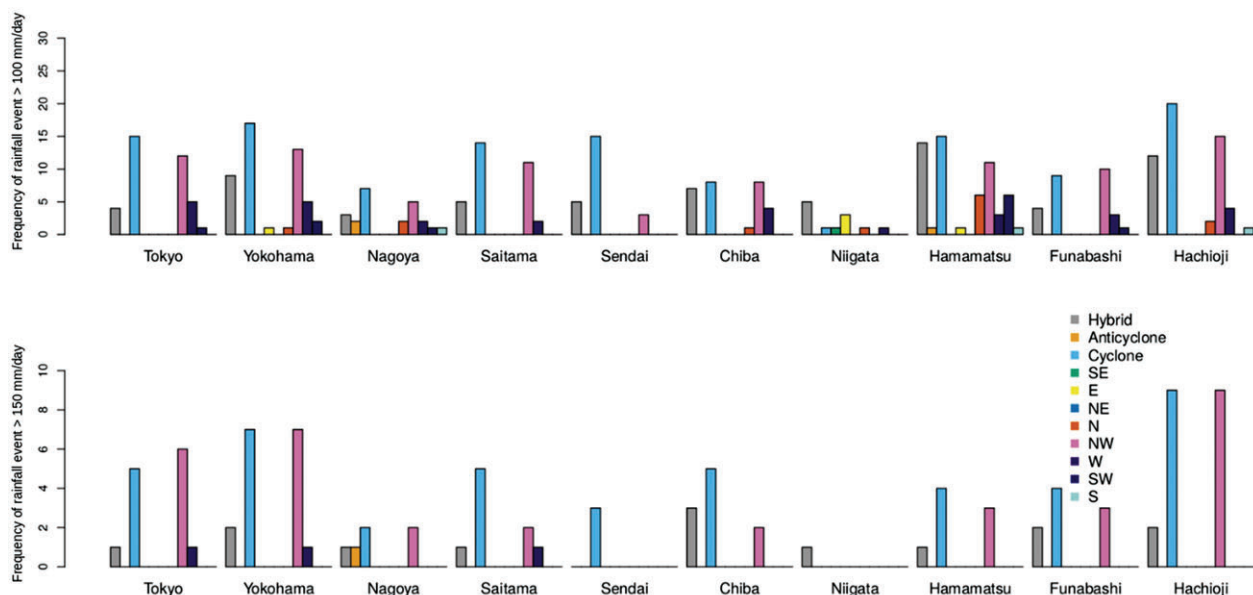

FIGURE 6 Frequency of extreme event per weather type at the meteorological stations located in major Japanese urban centres. (a) Frequency of event larger than 100 mm/day. (b) Frequency of event larger than 150 mm/day. From Vuillaume & Herath, 2016

TABLE 5 Date of events used for dynamic downscaling

C		H		NW		W	
Date	Cum. rain (mm)	Date	Cum. rain (mm)	Date	Cum. rain (mm)	Date	Cum. rain (mm)
October 06, 2014	123.5	September 17, 2015	74.5	October 13, 2014	49	October 05, 2014	148.5
October 16, 2013	176.5	September 09, 2015	156.5	June 06, 2014	123.5	October 15, 2013	69.5
May 03, 2012	121.5	July 03, 2015	67.5	September 15, 2013	78	January 14, 2013	64
September 21, 2011	124	December 03, 2010	76	April 04, 2013	53.5	August 05, 2008	111.5
September 08, 2010	102	October 27, 2007	88.5	August 10, 2009	111.5	December 26, 2006	154.5

In this study, we focused on the extreme rainfall events generated by the cyclone, hybrid, northwesterly and westerly wind weather types, respectively. We used the heaviest rainfall occurring between October 2006 and June 2016 recorded in the AMEDAS observation database station of Tokyo. Then, we retrieved the corresponding Global Forecast System (GFS) from National Oceanic and Atmospheric Administration (NOAA) archive data to pre-processed the WRF model. The Table 5 lists the case studies date used for the dynamical downscaling experiments.

3.2 | Dynamic Downscaling and regional rainfall forecast

Several publications emphasised on the optimisation of available micro-physics and cloud parametrisations to determine the best suitable combination for the location studied. We used the WRF version 3.8 model to predict the rainfall distribution intensity in the region around Tokyo area. The data provided by the GFS are used with a 3-hr interval. The data were ingested in the Weather Pre-processing System version 3.8. We did not investigate the effect of data assimilation system and the Weather Research and Forecasting Data Assimilation (WRFDA).

The model was simulated for 1 day and match the rainfall observation time recorded on the Japan AMEDAS gauge system at Japan Summer Time (JST). The Dynamical downscaling downscaled the GFS from about 55 km resolution to 27 km and 9 km. We used this resolution as a compromise between reaching the convection scale (<10 km) and took benefit of the cumulus scheme effect. Also, the limitation of computing power constrained the number of cases to be run ($24 \times 20 = 480$ simulations).

Moreover, this study used a 24 member ensemble as a combination of two Planetary Boundary, three micro-physics, two cumulus and two radiative scheme, respectively. The schematic Figure 7 illustrated the ensemble generation of the WRF optimisation schemes. Moreover, the Table 6 provided detail explanation regarding acronyms and literature reference to the physical schemes.

First, we designed the physical schemes with the average performance of 25 gauge stations around Tokyo (Location can be seen on Table 2). We identified the optimal scheme as the one who presents the lowest average rainfall error among five extreme events per weather type considered.

Therefore, we identified four optimal schemes, one per weather type. Then, a bias correction curve was computed using the WRF forecast result and the observation for the optimal scheme. Finally, we validated the corrective bias curve on 50 stations that are not part of the calibration pool.

3.3 | Bias correction

Bias correction has been used for rainfall forecast and climate modelling and projection for a long time. In both fields, rainfall is often underestimated by prediction model mainly due to coarse resolution and parametrisation, therefore, bias correction is necessary. However, rainfall climate change bias correction has got stronger attention expect for recent seasonal forecast bias correction. For this purpose, we used a classic gamma–gamma type correction as correction method to investigate the potential of the dynamics downscaling clustering methods.

The method used is based on the bias correction of the cumulative probability distribution of rainfall. The curve constructed based on 25 observation station is well approximated by a gamma–gamma function. Two curves are constructed, one for the observed rainfall and one for the WRF forecast rainfall. Then, corrective coefficients are derived from the corrections which are also correlated to the shape and scale of the rainfall described in the cluster rainfall definition. Therefore, correction curves are constraint by extreme rainfall signature which differs amount the cluster as seen previously on Figure 4.
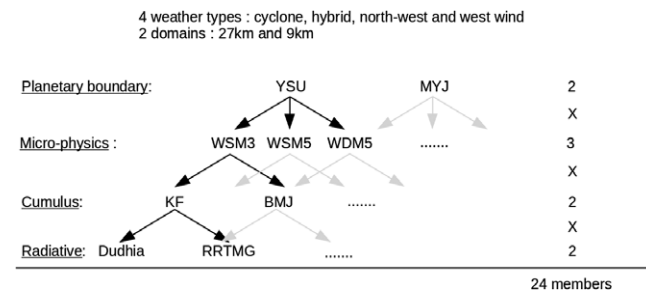

FIGURE 7 Weather research and forecasting (WRF) dynamical downscaling schemes optimisation tree. YSU, Yonsei University scheme; MYJ, Mellor-Yamada-Janjic scheme; WSM3, WRF single-moment 3-class scheme; WSM5, WRF single-moment 5 class scheme; WDM5, WRF double-moment 5-class scheme; KF, Kain-Fritsch scheme; BMJ, Betts-Miller Janjic scheme; Dudhia, Dudhia shortwave scheme; RRTMG, shortwave and longwave scheme

TABLE 6 Summary of the weather research and forecasting (WRF) parametrisations used in this work (from http://www2.mmm.ucar.edu/wrf/users/phys_references.html)

Label	Type	Description
YSU	Planetary boundary layer (PBL)	Yonsei University PBL scheme (Hong et al., 2006) Non-local diffusion scheme.
MYJ	PBL	Mellor-Yamada-Janjić Scheme, Viscous sublayer, and turbulence closure schemes (Janjić., 1994).
KF	Cumulus	Kain-Frisch cumulus scheme (Kain 2004). Mass-flux scheme able to accumulate CAPE.
BMJ	Cumulus	Betts-Miller-Janjic convection scheme (Janjic 2000). Deep layer control scheme unable to accumulate CAPE.
WSM3	Microphysics	WRF Single-Moment micro-physics parametrisation (Hong et al., 2004) with three species (vapour, cloud water/ice and rain/snow).
WSM5	Microphysics	Similar to WSM3 with two more species (vapour, cloud water, cloud ice, rain and snow are treated independently)
WDM5	Microphysics	CAM V5.1 two-moment five-class Scheme, Eaton, Brian (Lim & Hong., 2010).
Dudhia	Radiation	Numerical study of convection observed during the Winter. Monsoon Experiment using a mesoscale two-dimensional model (Dudhia., 1989).
RRTMG	Radiation	Radiative forcing by long-lived greenhouse gases Calculations with the AER radiative transfer models (Iacono., 2008).

We summarised below the steps used for bias correction:

1. We divided the rainfall stations into calibration (25) and validation (50) sets.
2. For both observed and forecast rainfall, we computed the shape and the scale of the rainfall for each cluster.
3. We estimated the correction coefficient by the one used to fit the forecast to the observed rainfall.
4. We assessed the performance of the correction on the validation set with rainfall root mean square error (RMSE) between 25 locations of AMEDAS station observation compared to interpolated WRF forecast outputs.

4 | RESULTS

The results obtained are discussed in two sections: (a) the scheme optimisation and calibration per weather type (b) the bias correction of weather type-based forecasts.

4.1 | Scheme optimisation and calibration

We performed an ensemble of 24 members WRF run tested on 20 extreme events case for a 1-day lead time forecast with a nested domain centred on the region of Tokyo. We used a 9-km grid resolution and included convective cumulus schemes. We compare the results of the WRF run with

observation station at 25 locations (see Figure 8) and the relative average error (in % of RMSE) for the ensemble of 25 stations estimated. The results obtained show a strong difference between weather absolute error larger than the variance of the absolute error among one weather type.

Our results suggest that weather type classification strongly influences the bias error. We notice that, variations among a weather type exist, but with limitation. The low variability of rainfall within a weather type is suggested by the low standard deviation value in Table 7. The table summarises the main results obtained from the scheme optimisation. Therefore, the average bias error for the cyclone, hybrid, northwesterly and westerly is estimated to 60.7, 34.2, 65 and 37.4%, respectively. We establish the optimal WRF result for each weather type such as YSU BMJ WSM3 Dudhia, MYJ KF WDM5 RRTMG, MYJ KF WSM5 Dudhia and YSU KF WSM5 Dudhia corresponding to C, H, NW and W weather type, respectively.

Also, we computed the ensemble score during single events such as the probability of schemes reaching rainfall above 50 mm/day. The result of the analysis is illustrated Figure 9. The shape of the rainfall pattern can be appreciated as well as the capacity of the majority of the physical schemes to predict similar events. Limited rainfall event present large difference subject to controversy area where probability rainfall is reaching only 50% such as C September 21, 2011, H September 17, 2015, H September 09, 2015. Moreover, it also indicated low-quality forecast of the GFS data as seen for the W August 04, 2008 event. Low probability of the ensemble, whereas 111.5 mm cumulative daily rainfall were recorded in Tokyo. However, it mainly gave indications on the quality of the schemes to reproduce an event in a consistent way.

Furthermore, we appreciated the weather type classification quality by the winds direction indicated in each figure. Therefore, westerly and northwesterly wind are well represented in the two last columns of the Figure 9. However, we performed weather type classification on a larger grid that encompasses the whole region of Japan. It is supposed to be valid at the scale of the region of south-east Japan as suggested by the Figure 9 in particular for NW and W wind. At the scale of cyclone and hybrid, we observed local wind direction organisation such as the H December 02, 2010 (local Southern winds). However, larger features confirmed a Hybrid weather type situation. This scheme optimisation analysis will later be used as a calibration step for the bias correction analysis later.

Finally, the Figure 10 illustrates the average performances of the bias correction. While both the cyclone and north-westerly bias correction highlight clear skills on 10a and 10c, other weather type seems to indicate limited potential of improvement (Figure 10b and d). Therefore, the Cumulative Probability Distribution Function bias error suffers from similar limitation as for the global correction
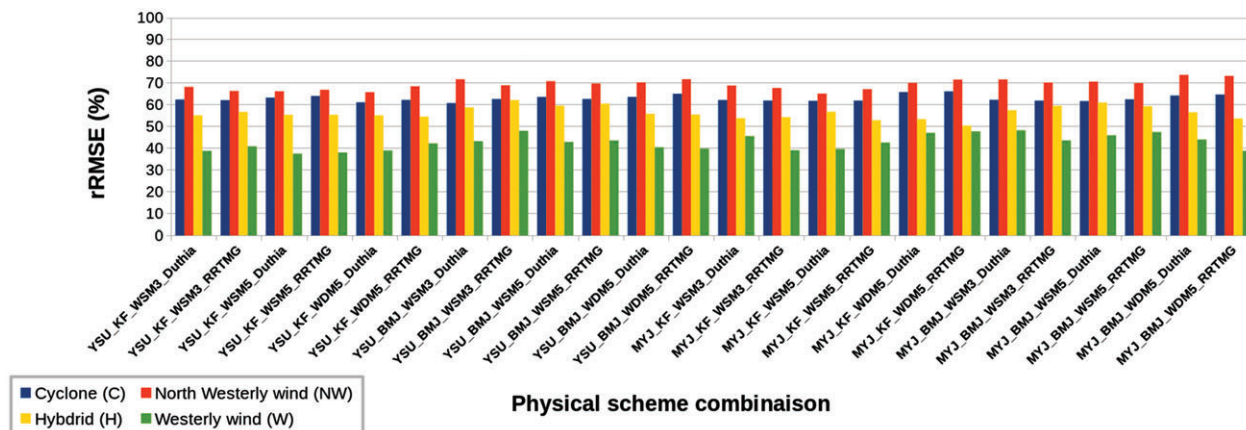
FIGURE 8 Graphical bar summary of the performance of forecast schemes in root mean square error (RMSE). Forecast performances are averaged for each weather type cluster. The yellow and green indicates the Cyclone (C), Hybrid (H), Northwesterly (NW) and Westerly wind (W), respectively

approach such that a positive average improvement validated by the Figures 8 and 10 does not necessary translate with individual stations improvement.

4.2 | Bias correction and validation

We used 50 station for validation of the bias correction. The bias correction curves are illustrated in Figure 10 and noted in 10a–d and were computed with 25 calibration stations. First, we can appreciated the difference between the bias correction curve. Both the cyclone (Figure 10a) and northwesterly (Figure 10c) present a corrective factor that increases with the rainfall. The cyclone curve presenting the higher bias as suggested by the Figure 10 and the summary Table 7. Moreover, the hybrid (Figure 10b) and westerly (Figure 10d) present both an inversion at about 80 mm that indicates a negative corrective bias error for rainfall below 80 mm/day and a positive bias correction for rainfall above 80 mm/day. The difference between the shape of the bias correction curve compared to raw WRF forecast advocates in the use of clustering method for optimisation that can give guideline in the (a) Optimal scheme to use (b) the construction of specific bias correction curves.

Figure 10 illustrates the result of the bias correction on the validation stations classified in cyclone (Figure 10e), hybrid (Figure 10f), northwesterly wind (Figure 10g) and westerly wind (Figure 10h). The result of the trend estimation is summarised in the Table 8. In general, a gain of the trend of 0–0.2 is observed that can indicate a gain of 0–20% in rainfall quantity correction. However, the average relative Root Mean Square Error (rRMSE) computation indicates an improvement of cyclone rainfall estimation of 17.8% while a quality decrease of all the others weather type (19.6, 8.5 and 8.1% for hybrid, northwesterly and westerly, respectively). This result indicates the limitation of a simple bias correction method based on cumulative PDF correction.

5 | DISCUSSION

5.1 | Classification methods

The weather type classification methods are practical and robust methods based on the wind direction and cyclonic/anticyclonic weather dynamic. Therefore, the weather type can easily be viewed with it rainfall distribution. However, this classification does not take into account the full complexity of the weather system which can be better captured by a multi-parameters approach such as a combination of (a) the bottom of the stratosphere ($\approx$200 hPa) and (b) the lower troposphere layer circulation and (c) the outgoing long-wave radiation (OLR) used for self-organised map described by the COST733 project: Harmonisation and Applications of Weather Type Classifications for European regions which conducted well documents reports and publication on the potential of weather typing for climate study. The project also involves the development of a weather type classification software over Europe using k-mean cluster classification based on multiple physical variable (COST, 2010). This approach was not tested in this research. However, Vuillaume (2015) discussed that LWT cluster Lamb (Lamb, 1972) presented a satisfying multi-parameters information classification. Moreover, specific humidity, temperature and mean velocity showed a similar pattern as the rainfall volume discussed Figure 5.

Further studies will be conducted to investigate the performance of self-organised map and bias correction method for weather forecasts. Results obtained by Moron, Robertson, Ward, and Ndiaye (2008) on climate bias correction of Global Climate Model give the indication of a "strong" potential of the method. It should be noticed that self-organised map required deeper regional atmospheric circulation understanding to appreciate it full value. Therefore, a comparison between the two classification systems should be investigated.
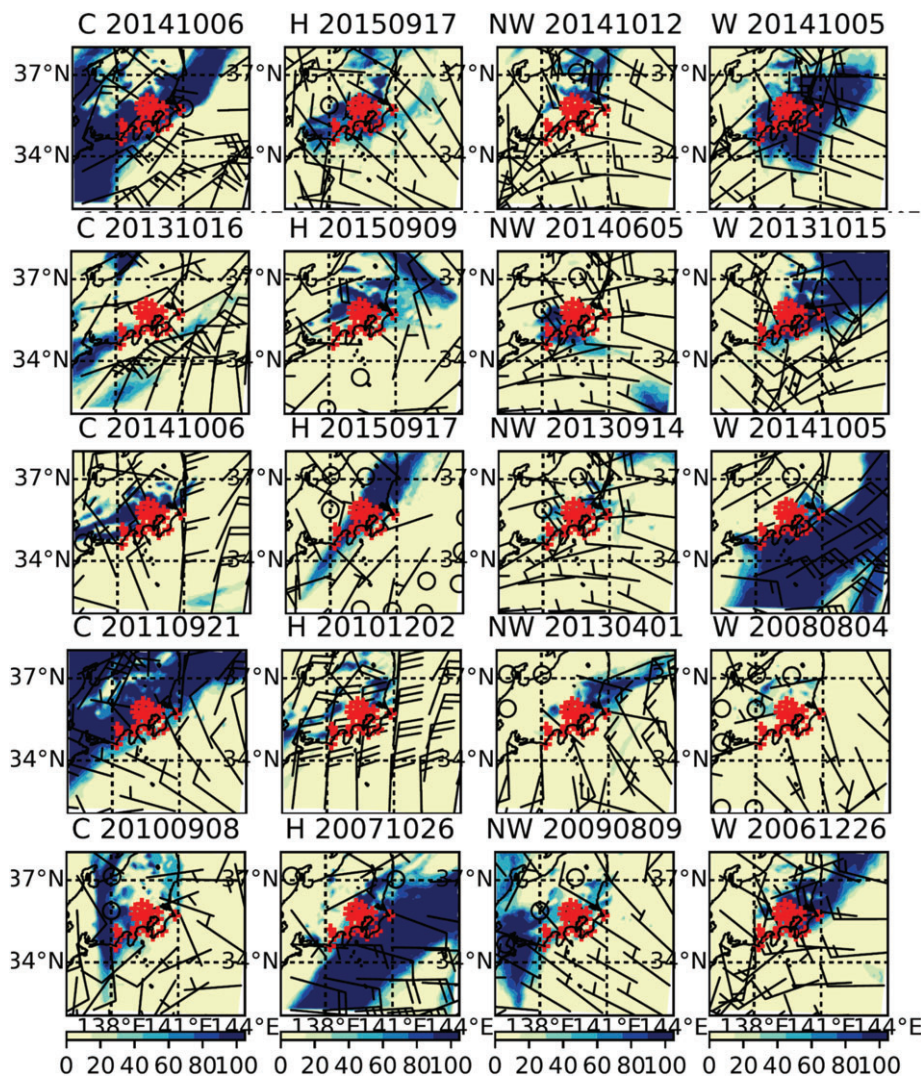
FIGURE 9 Ensemble rainfall forecast probability and mean wind direction forecast for the 20 extremes events date considered. The yellow to blue colour scale indicates a rainfall probability from 0 to 100% computed from the 24 ensemble forecast. For clarity, we classified the weather type in column and labelled them as C, H, NW and W with their respective date. The red cross indicates the station locations used for performance calibration. The arrow indicates wind direction and intensity like in common weather chart. A circle indicates a no wind preferences at that location

5.2 | WRF model

The WRF is a widely used NWP model which gives "acceptable" improvement of rainfall forecast estimation compared to the global models such as the NOAA and the ECMWF global model. However, the selection of the physical scheme is an expensive work, in particular for regions where weather is complex, such as Japan with usually a mid-latitude climate combined with seasonal tropical cyclones. The model experience continuous update of its physical scheme and therefore, new ones can always be subject to new study (For example, The WRF3.8 WRF version 3.8 presented a new Tiedke cumulus scheme, WRF manual).

We used the GFS data provided by the NOAA agency. We considered the ECMWF forecast data as an alternative. Furthermore, Vuillaume (2015) indicated that the ECMWF global rainfall forecast presented higher skills for rainfall prediction. However, the data provided by the ECMWF centre were not sufficient to able the WRF model to run dynamical downscaling.

High-Performance Computing system is required to create a large ensemble of case studies and increased the size of the physical ensemble. Therefore, this research addressed a limited number of physical schemes (24 members) that could be extended to enclose the most recent micro-physics, planetary Land Boundary and Cumulus schemes.

However, extreme rainfalls are limited events, in particular between 2006 and 2016 the range the available GFS data. Further, even more, limited weather situation are classified by small occurrences such as westerly. Therefore, westerly events which reached 100 mm/day were limited. Then, the extension of the number of cases will be limited, and we should considered a new GFS data set.

5.3 | Station-based performance

While the cyclone and northwesterly bias correction, highlight clear skills on Figure 10a, the hybrid and westerly weather type present very limited improvement (Figure 10b and d). Therefore, the Cumulative Probability Distribution Function bias error suffers from similar limitation as for the global correction approach such that a positive average improvement validated by the Figures 10 and 8 does not translate with individual stations improvement.
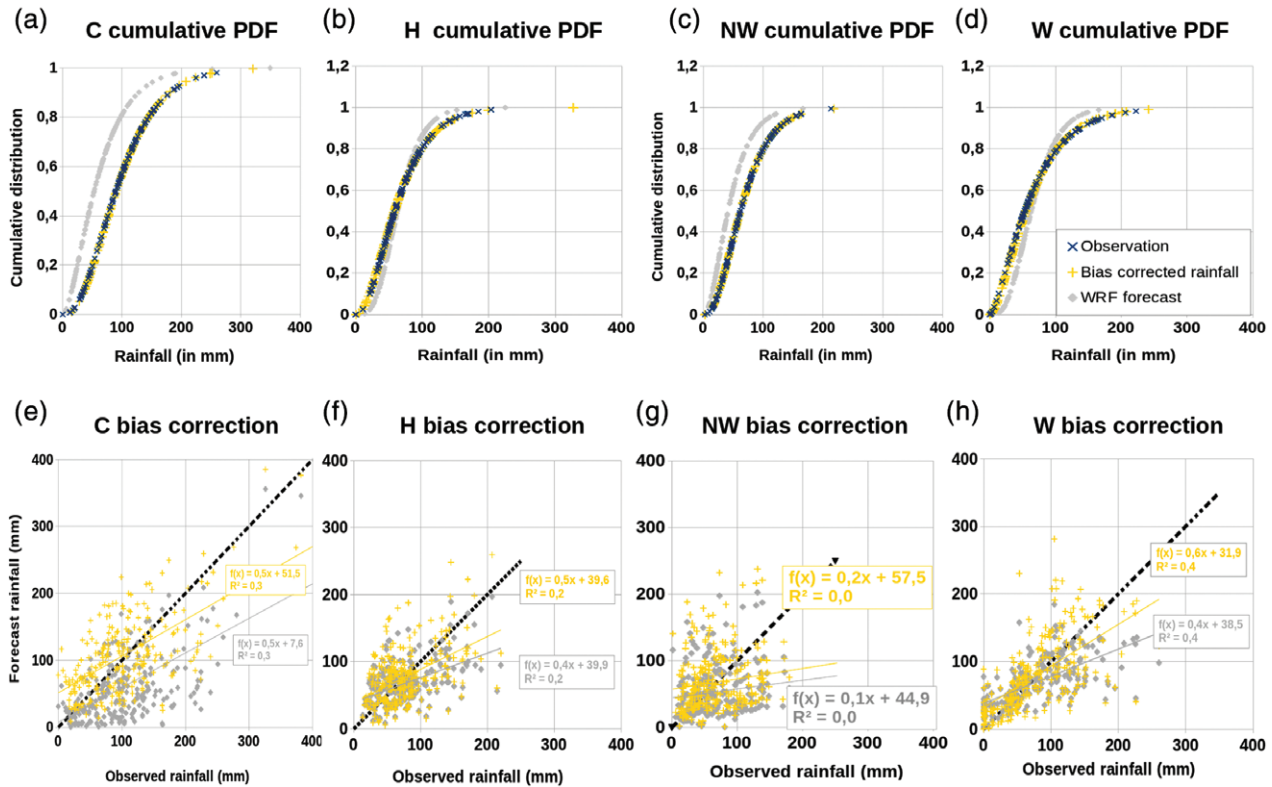
FIGURE 10 Illustration of the cumulative probability distribution function-based bias correction clustering for Cyclone (a), Hybrid (b), Northwesterly (c) and Westerly wind (d) weather type. The corresponding raw weather research and forecasting (WRF) forecast vs. bias corrected rainfall forecast is illustrated for C, H, NW and W in the subplot (e), (f), (g) and (h) respectively

TABLE 7 Summary results table of the root mean square error (RMSE) scheme optimisation classified per weather type

Weather type	Cyclone (C)	Hybrid (H)	North-west (NW)	West (W)
Optimal scheme	YSU BMJ WSM3 Dudhia	MYJ KF WDM5 RRTMG	MYJ KF WSM5 Dudhia	YSU KF WSM5 Dudhia
Absolute optimal RMSE scheme score (mm)	60.7	34.2	65	37.4
Absolute average score (%)	62.8	39.7	69.3	42.6
Absolute average standard deviation (%)	1.4	3.4	2.3	3.5

The evaluation of a pole of stations and the validation of this performance on another pool of stations is the central aspect of our optimisation scheme research. Hence, we evaluated the trends of the plots using observed vs. forecast. However, schemes performances can vary spatially due to local orography effect or the position of the station related, for example to the coastline and the sea. Also, we evaluated the performance of the bias correction spatially. Therefore, we focused our attention on the performance of the

TABLE 8 Linear trends coefficient from validation stations classified per weather type

Weather type	Cyclone (C)	Hybrid (H)	North-west (NW)	West (W)
WRF trend	0.5	0.4	0.1	0.4
Corrected trend	0.5	0.5	0.2	0.6
Average rRMSE reduction (in %)	−17.8	19.6	8.5	8.1

Note. RMSE = root mean square error; WRF, weather research and forecasting.

optimisation scheme per weather type on station (Figure 11 and 2, respectively) and therefore spatial distribution (Figure 12). For instance, further aspects of the correction were investigated such as the calibration and validation performance at single stations and the spatial distributions of the correction.

The Figure 11 illustrates the RMSE computed at each station individually for each weather type-based event. First, we observed wide disparities in performance between station for different weather type system which indicates a strong correlation between the stations and scheme optimisation method. Secondly, while cyclonic and northwesterly scheme remained the largest bias error weather type for the majority of stations, Oguchi and Kuki show that the broadest error is observed for hybrid. Westerly presented the lower rRMSE scheme for most of the station.

However, it is not possible to construct a good bias correction and optimised physical scheme at station based. First, for practicality, scheme optimisation has to be valid
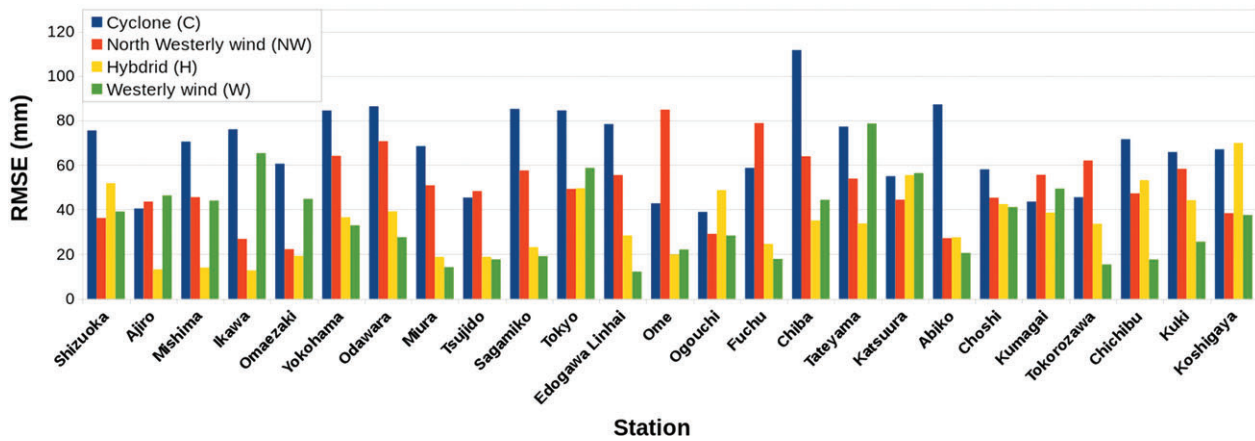
FIGURE 11 Graphical bar summary of the optimal physical scheme in root mean square error (RMSE) for each calibration stations. Forecast performances are average for each weather type cluster. The yellow and green indicates the Cyclone (C), Hybrid (H), Northwesterly (NW) and Westerly wind (W), respectively

for a domain since running competing forecast for each location will be costly. Also, bias correction curve required several and since extreme events are limited data available at one station will not be sufficient to build a calibration/validation model for explicit stations.

Also, we plot the spatial distribution of the calibration data for each weather illustrated by the Figure 12. We notice the distribution of the bias error in the south-east of Japan. Both cyclone (Figure 12a), hybrid (Figure 12b), northwesterly (Figure 12c) and westerly wind (Figure 12d) weather type present a strong homogeneous bias error in agreement with the bias correction curve illustrated Figure 10. Hence, cyclone weather types presents a large RMSE error for the majority of the stations, northwesterly weather types, presenting the lowest RMSE among the weather types, while the hybrid and westerly presents low to moderate RMSE with a larger spread than cyclone and northwesterly.

Finally, the Figure 12 illustrates the performances of the bias correction. While the cyclone bias correction highlight clear skills on 12a. Other weather type presents clear localised improvement on East part of Kanto area (Figure 12b), slight quality decrease (Figure 12c) and a mix behaviour (Figure 12d). Therefore, the Cumulative Probability Distribution Function bias error suffers from similar limitation as for the global correction approach. A positive average improvement validated by the Figure 8 and the Figure 10 does not translate with individual stations improvement. We should, therefore, investigate a bias correction method that could take into account larger spatial disparity in weather systems such as a predictant–predictors approach method (Statistical DownScaling Model, SDSM by Wilby & Dawson, 2013) and the empirical statistical downscaling by Benestad (2010). Furthermore, current weather forecast suffer from limitation in their physics parametrisation and
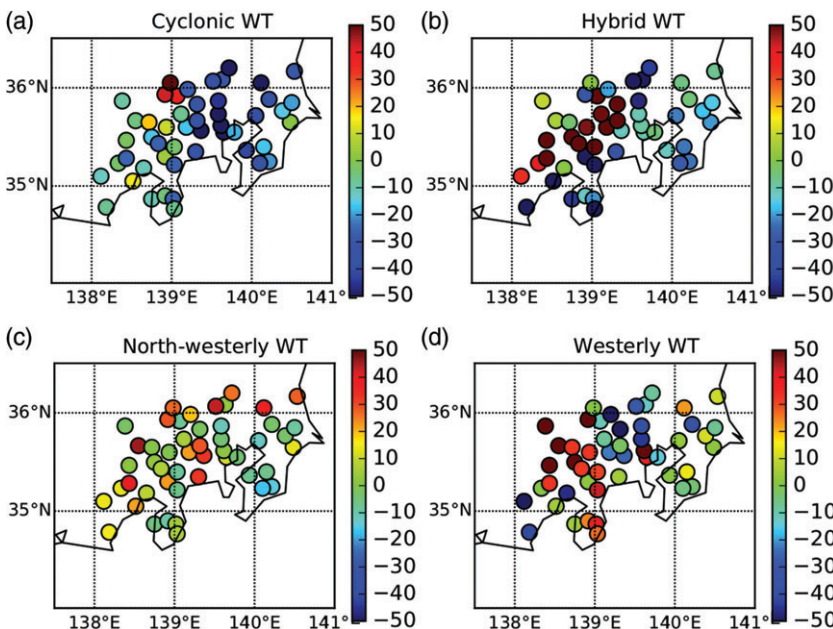

FIGURE 12 Spatial distribution of the absolute root mean square error difference between weather research and forecasting raw forecast and bias corrected forecast (in %). We considered the validation stations classified for Cyclone (a), Hybrid (b), North-westerly (c) and Westerly (d) events. Blue, yellow and red indicates a low, intermediate and large absolute bias error, respectively

grid spacing that still lead to bias error when compared to observation station.

6 | CONCLUSIONS

In this study, we (a) estimate an optimal physical scheme for each cluster (b) improve regional rainfall forecast by the use of bias correction curves divided by weather type and (c) evaluate the spatial variability of the bias correction. This research links the weather cluster selection with a particular scheme and a particular rainfall bias correction. Therefore, the results of this study recommend that, bias correction can be partially corrected by taken advantage of weather type classification.

We used 25 stations for the calibration and 50 stations for the validation of the bias correction. We showed the improvements obtained by the performance of the scheme over several events and a pool of stations. However, we focused on bias correction of extreme rainfall events in a limited regional area and therefore stations showed a strong variability in the optimisation of the scheme. Then, it also affects the performance of scheme for other events than cyclone system. Therefore, the following research should focus on the bias correction methods and how to adapt it to either specific stations or either used more complex bias corrective methods.

Bias correction improves the quality of all the trend between observed and forecast rainfall for each cluster by about 10–20% depending on weather type. However, rRMSE indicates that only the cyclone weather type improve by 20%. In addition, the bias reduction is mainly located east side of Kanto area. The hybrid weather type present strong localisation of improvement but resulting with a global decrease of rainfall quality. For instance East and South part were strongly improve while North West of Kanto strongly degraded. The North westerly while presenting promising potential based on the cumulative bias correction curve (Figure 10) present a global and local degradation (Table 8 and Figure 12). The Westerly weather type exhibit complex responses to the correction that indicate a slight improvement at the central area but strong degradation westward of the Kanto area, other region being unchanged.

Finally, we raised future questions by this study. First, seasonal variation of weather type occurrence could be investigated to determine its trends and add further value to the forecast. Second, others region should be tested with similar methods to confirm the potential of the method. Third, we should investigate the impact of rainfall forecast improvement on an operational flood alert system.

6.1 | Code availability

The WRF code is an open source code available at http://www2.mmm.ucar.edu/wrf/users/download/get_source.html

6.2 | Data availability

All AMEDAS and GFS data are on public domain and can be on JMA (http://www.jma.go.jp) and NOAA website (https://www.ncdc.noaa.gov/data-access/model-data/model-datasets/global-forcast-system-gfs).

ORCID

J.-F. Vuillaume http://orcid.org/0000-0002-8136-3481

REFERENCES

Baltaci, H., Göktürk, O., Kindap, T., Ünal, A., & Karaca, M. (2014). Atmospheric circulation types in Marmara Region (NW Turkey) and their influence on precipitation. *International Journal of Climatology*, *35*(8), 1810–1820.

Benestad, R. E. (2010). Downscaling precipitation extremes. *Theoretical and Applied Climatology*, *100*, 1–21. https://doi.org/10.1007/s00704-009-0158-1

Bower, D., McGregor, G. R., Hannah, D. M., & Sheridan, S. C. (2007). Development of a spatial synoptic classification scheme for western Europe. *International Journal of Climatology*, *27*, 2017–2040. https://doi.org/10.1002/joc.1501

Calvo, A., Pont, V., Olmo, F., Castro, A., Alados-Arboledas, L., Vicente, A., … Fraile, R. (2012). Air masses and weather types: A useful tool for characterizing precipitation chemistry and wet deposition. *Aerosol and Air Quality Research*, *12*, 856–878.

COST (2010). COST733 harmonisation and applications of weather type classifications for European regions. Retrieved from http://cost733.geo.uni-augsburg.de/cost733wiki.

Dudhia, J., (1989). Numerical study of convection observed during the Winter Monsoon Experiment using a mesoscale two–dimensional model. *J. Atmos. Sci.*, *46*, 3077–3107.

Evans, J. P., Ekström, M., & Ji, F. (2012). Evaluating the performance of a WRF physics ensemble over South-East Australia. *Climate Dynamics*, *39*, 1241–1258. https://doi.org/10.1007/s00382-011-1244-5

Gilmore, J. B., Evans, J. P., Sherwood, S. C., Ekström, M., & Ji, F. (2016). Extreme precipitation in WRF during the Newcastle East Coast low of 2007. *Theoretical and Applied Climatology*, *125*, 809–827. https://doi.org/10.1007/s00704-015-1551-6

Hayasaki, M., & Kawamura, R. (2012). Cyclone activities in heavy rainfall episodes in Japan during spring season. *SOLA*, *8*, 45–48. https://doi.org/10.2151/sola.2012-012

Hess, P., & Brezowsky, H. (1952). *Berichte des Deutschen Wetterdienst in der US-Zone 33*. Bad Kissingen: Deutscher Wetterdienst, DWT.

Hong, Song-You, Jimy, Dudhia, and Shu-Hua, Chen (2004). A revised approach to ice microphysical processes for the bulk parameterization of clouds and precipitation. *Mon. Wea. Rev.*, *132*, 103–120.

Hong, S., Noh, Y., and Dudhia, J. (2006). A New Vertical Diffusion Package with an Explicit Treatment of Entrainment Processes. *Mon. Wea. Rev.*, *134*, 2318–2341. https://doi.org/10.1175/MWR3199.1

Huth, R., Beck, C., Philipp, A., Demuzere, M., Ustrnul, Z., Cahynová, M., … Tveito, O. E. (2008). Classifications of atmospheric circulation patterns: Recent advances and applications. *Annals of the New York Academy of Sciences*, *1146*, 105–152.

Iacono, M. J., Delamere, J. S., Mlawer, E. J., Shephard, M. W., Clough, S. A., and Collins, W. D. (2008). Radiative forcing by long–lived greenhouse gases: Calculations with the AER radiative transfer models. *J. Geophys. Res.*, *113*, D13103.

Islam, T., Srivastava, P. K., Rico-Ramirez, M. A., Dai, Q., Gupta, M., & Singh, S. K. (2015). Tracking a tropical cyclone through WRF–ARW

simulation and sensitivity of model physics. *Natural Hazards*, *76*, 1473–1495. https://doi.org/10.1007/s11069-014-1494-8

Janjić, Z. I. (1994). The Step-Mountain Eta Coordinate Model: Further Developments of the Convection, Viscous Sublayer, and Turbulence Closure Schemes. *Mon. Wea. Rev.*, *122*, 927–945. https://doi.org/10.1175/1520-0493(1994)122<0927:TSMECM>2.0.CO;2

Janjić, Z. I. (2000). Development and Evaluation of a Convection Scheme for Use in Climate Models. *J. Atmos. Sci.*, *57*, 3686–3686. https://doi.org/10.1175/1520-0469(2000)057<3686:CODAEO>2.0.CO;2

Jankov, I., Gallus Jr., W. A., Segal, M., Shaw, B., & Koch, S. E. (2005). The impact of different WRF model physical parameterizations and their interactions on warm season MCS rainfall. *Weather and Forecasting*, *20*, 1048–1060. https://doi.org/10.1175/WAF888.1

Jenkinson, A., & Collison, F. (1977). An initial climatology of gales over the North Sea. Synoptic Climatology Branch, Memorandum, 62, UK Met Office, Bracknell.

Ji, F., Ekström, M., Evans, J. P., & Teng, J. (2014). Evaluating rainfall patterns using physics scheme ensembles from a regional atmospheric model. *Theoretical and Applied Climatology*, *115*, 297–304. https://doi.org/10.1007/s00704-013-0904-2

Japanese Meteorological Agency (JMA) (2017). Kanto and Koshin seasonal meteorology. Retrieved from www.data.jma.go.jp/gmd/cpd/lonfcst/en/tourist/file/Kanto_Koshin.html.

Jones, P. D., Hulme, M., & Briffa, K. R. (1993). A comparison of lamb circulation types with an objective classification scheme. *International Journal of Climatology*, *13*, 655–663.

el Kenawy, A. M., McCabe, M. F., Stenchikov, G. L., & Raj, J. (2014). Multi-decadal classification of synoptic weather types, observed trends and links to rainfall characteristics over Saudi Arabia. *Frontiers in Environmental Science*, *2*:37. https://doi.org/10.3389/fenvs.2014.00037

Lamb, H. (1972). *British Isles Weather Types and a Register of Daily Sequence of Circulation Patterns, 1861–1971, Geophysical Memoir 116*. London: HMSO.

Lee, C. C., & Sheridan, S. C. (2012). A six-step approach to developing future synoptic classifications based on GCM output. *International Journal of Climatology*, *32*, 1792–1802.

Moron, V., Robertson, A. W., Ward, M. N., & Ndiaye, O. (2008). Weather types and rainfall over Senegal. Part I: Observational analysis. *Journal of Climate*, *21*, 266–287. https://doi.org/10.1175/2007JCLI1601.1

Riediger, U. and Gratzki, A., (2014). Future weather types and their influence on mean and extreme climate indices for precipitation and temperature in Central Europe. *Meteorologische Zeitschrift*, *23*, 231–252. https://doi.org/10.1127/0941-2948/2014/0519

Rousi, E., Mimis, A., Stamou, M., & Anagnostopoulou, C. (2014). Classification of circulation types over Eastern Mediterranean using a selforganizing map approach. *Journal of Maps*, *10*, 232–237.

Skamarock, W. C., Klemp, J. B., Dudhia, J., Gill, D. O., Barker, D. M., Duda, M. G., … Powers, J. G. (2008). A Description of the Advanced Research WRF version 3, NCAR Technical Note NCAR/TN-475+STR.

Trigo, R. M., & DaCamara, C. C. (2000). Circulation weather types and their influence on the precipitation regime in Portugal. *International Journal of Climatology*, *20*, 1559–1581. https://doi.org/10.1002/1097-0088(20001115)20:13<1559::AID-JOC555>3.0.CO;2-5

Vuillaume, J.-F. (2015). *Optimization of flood early warning by rainfall forecast improvement*. (PhD thesis). United Nations University, Institute for Sustainability and Peace (pp. 156).

Vuillaume, J.-F., & Herath, S. (2016). Improving global rainfall forecasting with a weather type approach in Japan. *Hydrological Sciences Journal*, *62*(2), 167–181. https://doi.org/10.1080/02626667.2016.1183165

Wilby, R. L., & Dawson, C. W. (2013). The statistical downscaling model: Insights from one decade of application. *International Journal of Climatology*, *33*, 1707–1719. https://doi.org/10.1002/joc.3544